Applied Thermal Engineering 232 (2023) 121015

Contents lists available at ScienceDirect

Applied Thermal Engineering

journal homepage: www.elsevier.com/locate/ate

Research Paper

Thermodynamic analysis of stratification in thermal energy storages implemented in cogeneration systems

B. Thomas [a,*], P.D. van Schalkwyk [b], J.A.A. Engelbrecht [b], P. Haase [a], A. Maier [a], C. Widmann [a], M.J. Booysen [b]

[a] Reutlingen Energy Center (REZ), Reutlingen University, Germany
[b] Department of E&E Engineering, Stellenbosch University, South Africa

ARTICLE INFO

Keywords:
Thermal stratification
Stratification indices
CHP unit
Cogeneration
Thermal energy storage
Exergy analysis

ABSTRACT

In the course of a more intensive energy generation from regenerative sources, an increased number of energy storages is required. In addition to the widespread means of storing electric energy, storing energy thermally can contribute significantly. However, limited research exists on the behaviour of thermal energy storages (TES) in practical operation. While the physical processes are well known, it is nevertheless often not possible to adequately evaluate its performance with respect to the quality of thermal stratification inside the tank, which is crucial for the thermodynamic effectiveness of the TES. The behaviour of a TES is experimentally investigated in cyclic charging and discharging operation in interaction with a cogeneration (CHP) unit at a test rig in the lab. From the measurements the quality of thermal stratification is evaluated under varying conditions using different metrics such as normalised stratification factor, modified MIX number, exergy number and exergy efficiency, which extends the state of art for CHP applications. The results show that the positioning of the temperature sensors for turning the CHP unit on and off has a significant influence on both the effective capacity of a TES and the quality of thermal stratification inside the tank. It is also revealed that the positioning of at least one of these sensors outside the storage tank, i.e. in the return line to the CHP unit, prevents deterioration of thermal stratification, thereby enhancing thermodynamic effectiveness. Furthermore, the effects of thermal load and thermal load profile on effective capacity and thermal stratification are discussed, even though these are much smaller compared to the effect of positioning the temperature sensors.

1. Introduction

At the Paris UN Climate Change Conference in 2015 it was jointly agreed to limit global warming to a rise of temperature below 2 °C, or better still below 1.5 °C, compared to pre-industrial levels [1]. At the 2021 Climate Conference in Glasgow, this decision was reaffirmed, and further measures such as halting the destruction of forests and reducing methane emissions were agreed [2]. However, the main focus remains on phasing out the burning of fossil fuels to provide secondary energy in the heat, electricity and transportation sectors. Many countries have therefore set targets for switching to renewable energies. The EU aims to reduce greenhouse gas emissions by at least 55 % by 2030 compared to the 1990 baseline [3]. The USA announced a reduction of greenhouse gas emissions by at least 50 % by 2030 compared to 2005 levels [4], and China wants to be climate neutral by 2060 [5].

Looking at the measures and the success that have been initiated and achieved so far, it becomes clear that the transformation in the electricity sector has already progressed considerably further than in the heat and transportation sectors, essentially by the construction of PV and wind power plants. In order to increase the share of renewable energies in the heat and transportation sectors as well, it is necessary to couple the sectors, or in other words to transfer the electricity generated by PV and wind power plants to the heat and transportation sectors. In the latter sector, major efforts are currently being made to introduce electromobility. In the heat sector, there is an increased focus on heat pumps. Another type of sector-coupling is provided by cogeneration, where waste heat from electricity generation is utilised for heating purposes. Since the chemical energy in the fuel is more comprehensively converted into electric power and useful heat, a higher fuel efficiency is achieved. If, in addition, a CO_2-neutral fuel such as biogas or green hydrogen is used, cogeneration can serve as a highly efficient, carbon neutral technology for providing both electricity and useful heat.

In any sector-coupling technology, the use of energy storage systems is indispensable to synchronise the generation and consumption of

* Corresponding author.
E-mail address: bernd.thomas@reutlingen-university.de (B. Thomas).

https://doi.org/10.1016/j.applthermaleng.2023.121015
Received 11 October 2022; Received in revised form 1 May 2023; Accepted 16 June 2023
Available online 20 June 2023

Nomenclature

c_p	Specific heat capacity $\left[\frac{\mathrm{J}}{\mathrm{kgK}}\right]$
D	Diameter [m]
E, Q	Energy, Heat [J]
Ex	Exergy [J]
Ex^*	Exergy number [−]
g	Gravitational acceleration $\left[\frac{\mathrm{m}}{\mathrm{s}^2}\right]$
H	Height of the TES [m]
J	Number of layers [−]
M_E	Moment of energy [J · m]
MIX	MIX number [−]
MIX*	Normalised MIX number [−]
Pe	Peclet number [−]
Ri	Richardson number [−]
ST	Stratification factor [K^2]
ST^*	Normalised ST factor [−]
Str	Stratification number [−]
t	Time, [s]
TC	Thermocouple
T_j	Temperature at node j [°C]
V	Volume [m^3]
$\dot{V}$	Volumetric flow rate $\left[\frac{\mathrm{m}^3}{\mathrm{s}}\right]$
y	Vertical distance [m]
$\tilde{y}$	Distance to layer centre node [m]
α	Thermal diffusivity $\left[\frac{\mathrm{m}^2}{\mathrm{s}}\right]$
β	Coefficient of thermal expansion [1/K]
Δt	Sampling period [s]
$\partial z, \Delta z$	Change in vertical distance [m]
η	Efficiency [−]
ρ	Density $\left[\frac{\mathrm{kg}}{\mathrm{m}^3}\right]$
υ	Fluid velocity $\left[\frac{\mathrm{m}}{\mathrm{s}}\right]$

Subscripts

bot	Bottom of tank
cold	Cold region
eff	Effective
fully-mixed	Fully-mixed case
hot	Hot region
ideal-str	ideally-stratified case
in	Inlet
j	Layer or node number
m	Mixed or Bulk mean
max	Maximum
min	Minimum
t	At a specific time
tank	The TES tank
TES	Thermal energy storage tank
top	Top of tank

the different forms of energy. When coupling the electricity and heat sectors, as in the case of cogeneration, it is often beneficial to use a thermal energy storage (TES) with water as the storage medium, usually labelled as hot water tank. This method of energy storage is less expensive than electrical energy storage systems. Moreover, such tanks are often mandatory to decouple thermal generation from fluctuations of the current heat demand in time, and therefore they usually form an integral part of cogeneration plants and heat pump systems anyway.

Despite the benefits of thermal energy storages, their efficient use is constrained by limited understanding of the exact thermodynamic properties inside the tank. Therefore, in many cases basic "rule of thumb" methods are applied to estimate a good size of the hot water tank acting as thermal energy storage. For a better understanding, the distribution of temperatures especially in vertical direction is of interest, due to the fact that hot water rises because of its lower density, while cold water descends accordingly. This is known as thermal stratification. Besides the practical aspects of this phenomenon, it is also important in terms of thermodynamic effectiveness of the TES. A perfectly stratified storage tank with a hot water zone in the top and a cold water zone at the bottom, is thermodynamically more valuable than an isothermal TES at constant mixing temperature, although the content of energy is the same in both cases. Thermodynamically, this effect is expressed by exergy, and for that reason exergy will be one of the metrics applied in the following for evaluating the quality of thermal stratification in thermal energy storages.

Another reason why thermal stratification in the TES of cogeneration and heat pump installations is of special interest is the fact that the temperatures inside are measured at different locations, or more specifically different heights, for turning the CHP and heat pump units on and off. Hence, it is important to know what fractions of the entire energy stored in the tank are located above and below the temperature sensor for controlling the units. In other words, the vertical temperature distribution in the tank is an important measure for the functional and efficient operation of these systems. Moreover, since demand-oriented operation is heavily dependent on the ability of cogeneration units (CHP units) and heat pumps to efficiently match generation with consumption, the thermal energy storage is a key element in the entire installation, further emphasising the need for a good understanding of its thermodynamic behaviour [6,7].

To address this challenge, the thermal stratification was experimentally investigated and analysed in a TES as part of a cogeneration plant. In particular, the research questions are how different operating modes of a CHP unit affect thermal stratification in the TES, how this affects its thermodynamic effectiveness, and what metrics are appropriate for accurately evaluating the quality of thermal stratification in this application. For this purpose, various experiments were carried out on a TES connected to a small CHP unit. Subsequently, the results were evaluated with regard to thermal stratification in the TES using different metrics to derive its thermodynamic effectiveness. This finally serves to answer the research questions in both aspects: It will become clear what kind of metrics are suited to evaluate thermal stratification and, through this means the thermodynamic effectiveness of a TES in a CHP installation. In addition, the results will reveal the effects of the parameter varied during CHP operation on thermal stratification in the TES. These answers constitute the novelty and originality of the publication compared to the existing literature, as will be shown in the next section.

The structure of this paper is as follows: In Section 2, various works from the existing scientific literature dealing with the analysis of thermal stratification in thermal energy storages are collated and evaluated to form a basis for the analysis. Section 3 describes the experimental setup at the test stand. Section 4 is devoted to the various metrics and criteria found in the literature for characterising the thermodynamic quality of thermal stratification in a TES. At the end of the section, the criteria applicable for an installation comprising a CHP unit in combination with a TES are identified. After illustrating the experimental procedure in Section 5, the test results are explained and evaluated in Section 6 based on the criteria elaborated beforehand. A conclusion finalises the publication in Section 7.

2. Related work

When comparing different TES devices on the market, it is desirable to have and use numerical indices to determine the ability of a TES

to promote and maintain thermal stratification during charging, storing and discharging processes [8]. The performance characterisation of TES devices, with respect to thermal stratification, requires the implementation of a variety of indices that are obtained from literature.

Haller, et al. [8] provided an extensive review of different methods that have been proposed in literature to characterise thermal stratification in TES devices. These methods specifically focussed on determining the effect of stratification using single numerical values that can be useful when comparing different experimental cases. The authors highlighted the importance of distinguishing between factors that influence the degree of stratification and the numerical numbers that are generally used to characterise stratification. Factors that influence the degree of stratification include the height of the tank and its relation to the tank diameter, the inlet water temperature and the flow rate of the discharging water. The authors concluded that not all characterising metrics are equally applicable to all three processes of charging, discharging and storing [8]. For example, indices such as the stratification coefficient, ST, and the thermocline thickness both require internal temperature measurements of the TES and provide an appropriate indication of the quality of stratification for all three processes as mentioned before, however, a metric such as the discharge/charging efficiency number is not applicable for purely storing processes.

González-Altozano, et al. [9] presented a method, termed the virtual thermocouple (TC) method, which allows water temperature to be estimated at any depth and at any time during a TES charging process. During the formulation of this method, the five-parameter logistic (5PL) function was applied to fit and estimate the sigmoidally-shaped temporal trend that was observed for each measured node. The experimental data was collected from a test bench comprising a 905 litres vertical TES tank with a 0.8 m diameter and a height of 1.8 m. The temperatures along the height of the tank were recorded using 12 type-T thermocouples that were installed equally-spaced along the height of the tank. In addition, two more thermocouples were used to measure the inlet and outlet temperature. Two independent and geometrically-varying inlet ports were arranged at the top of the tank in-line with its vertical axis — a conventional inlet elbow and a sintered bronze conical diffuser. Four experiments were conducted, a low flow rate of 6 litres/min and a high flow rate of 16 litres/min for each of the two inlet configurations. The results of the Virtual TC method showed an appropriately-fitted model for the internal temporal trends. The average RMSE value for the elbow inlet configuration model was shown to be 0.5075 °C for low flow rate and 0.9523 °C for high flow rates. The average RMSE values for the conical diffuser inlet configuration model was 0.2374 °C for low flow rate and 0.4197 °C for high flow rates.

Gasque, et al. [10] conducted a study where the characterisation of internal temporal trends in a TES was investigated with the aim of minimising the number of thermocouples used for model development. Their study was an extension on the work that was done in González-Altozano, et al. [9]. More specifically, this study was focused on assessing the sensitivity of the Virtual TC method as defined in González-Altozano, et al. [9] and how it could be used to determine the minimum number of thermocouples needed for accurate characterisation. Using the existing data from González-Altozano, et al. [9], four additional models were developed for each of the four experiments. These models were each developed with fewer and a decreasing number of thermocouples — 7 TCs, 4 TCs, 3 TCs and 2 TCs. From the results it was concluded that models developed using fewer number of thermocouples, such as 7 TCs, 4 TCs and 3 TCs, showed a similar temporal patterns to the former 12 TCs models. The RMSE values for all models were on average less than 0.6 °C.

Fernández-Seara, et al. [11] investigated the degree of thermal stratification within a 150 litres vertically-oriented tank with a heating element located at the bottom. The tank was installed with 11 temperature sensors positioned along the height of the tank to a probe depth of 20 cm. The study introduced six different inlet-outlet configurations and three different flow rates (5, 10, and 15 litres/min) as experimental parameters. From their results, it is clear that the inlet-outlet port configuration has a significant impact on the development of the internal temporal trend as a function of time. This was also observed in the studies by González-Altozano, et al. [9] and Gasque, et al. [10]. The stratification number, Str, was first defined in part 1 of this study and was used as a stratification metric to compare the different experiments with one another. Based on the results in the form of stratification number, it was evident that low flow rates promoted better thermal stratification, while high flow rates caused more turbulence and, as a result, more mixing. This was observed and discussed in other studies in literature [8,10,12–14].

Castell, et al. [13] compared a variety of characterisation numbers for thermal stratification and general efficiency for a vertically-oriented TES tank. The experimental setup consisted of a TES device with a volume of 287 L, a height of 1.56 m and a diameter of 0.5 m. The temperatures along the height of the TES were measured using six equally-spaced PT100 temperature sensors. The study used a variety of dimensionless characterisation numbers, such as the MIX number, Richardson number, discharge efficiency, Peclet number and the Reynolds number. One of the study's conclusions was that the Peclet and Reynolds numbers were not suitable for thermal stratification characterisation. They further concluded that the working flow rate and the working temperature, also known as the set or target temperature, were typically the most influential variables affecting the stratification in their study. The MIX number and Richardson numbers were considered to be appropriate metrics for characterising stratification. However, it was noticeable that the MIX number was sensitive to small temperature changes in device set temperatures.

Van Schalkwyk, et al. [14] developed an experimental platform for a horizontally-oriented, domestic electric water heater (DEWH). The aim of the study and platform was to measure the internal temperature profile development and to characterise the thermal stratification for numerous environmental and operational cases. The TES tank had a volume of 150 litres and was sectioned at the inlet side to envelope a separate thermal stratification measurement unit with 66 temperature sensors. The study showed measured results that provided three-dimensional temperature variation for heating, storing and discharging experiments, including the thermal stratification in the vertical axis, which was sectioned into 9 measured layers. The results provided observations that the most prominent temperature variation occurred in the vertical axis, owing to thermal stratification, and that there was little to no temperature variation along the length of the tank, except at the inlet port of the tank. It was also observed that the lower region of the tank remained remarkably colder than the upper layers during the thermal charging phase. A temperature difference between the bottom layer temperature and the thermostat temperature was measured to be at least 30 °C at the time the thermostat measured a temperature of 60 °C and switched off. The authors concluded that the three lower layers of the tank have a significantly slower thermal response when compared to the upper layers and could possibly remain within a crucial temperature range, conducive for pathogenic growth, such as *Legionella pneumophila*.

Celador, et al. [15] assessed different stratification modelling strategies for TES devices that were used as buffer tanks in Combined Heat and Power (CHP) plants. More specifically, the aim was to study the effect of applying different models for energetic and economic simulations of CHP units based on internal combustion engines. Three different models for three TES stratification cases were studied and applied — an actual stratified tank, an ideally-stratified tank and a fully-mixed tank. The authors stated that thermal stratification not only influences the exergy efficiency of the TES, but also the global performance of the CHP plant. Also, mixing does not directly imply energy losses, but more exergy destruction since the heat transfer between the components of the plant is affected. The data from a case study using a CHP plant, located in Bilbao metropolitan area in Spain, was used to perform the comparison between the three models. The residential

area had an annual heat demand for heating and hot water usage. The thermal efficiencies of the storage tank were 95.60 %, 92.87 %, and 89.16 % for ideal stratification, actual stratification, and fully-mixed models, respectively. Interestingly, these three stratification cases were also used when calculating the MIX number as shown in this and other studies [8,12,13].

Wang, et al. [16] conducted a study on the influence of a custom-designed, inlet-fitted equaliser on the performance of thermal stratification in a 60 L TES installed in a solar plumbing configuration. The TES tank also had an additional 1.5 kW heating element for resistive heating. The tank was probed with 16 PT100 temperature sensors at a radial depth of 100 mm. The aim of the study was to determine the influence of the TES inlet modes on the thermal stratification performance and fill efficiency (a stratification performance index defined in this study). The experimental tests were conducted with various flow rates ranging from 1 L/min to 6 L/min. Apart from the experimental results, a CFD model was also generated using ANSYS. The results from the experiments and the CFD model were used in conjunction with common stratification indices, such as Richardson number, MIX number and exergy efficiency. The results of the study showed that the inlet equaliser had a positive effect on the stratification conservation in the tank and that the CFD model was in good agreement with the experimental results. The authors concluded that the flow rate is one of the most important influential factors during a thermal charging process. This is corroborated by other studies [9,10,12,16].

Maruf, et al. [17] provided a detailed review of current power to heat (P2H) and energy storage technologies and classified them according to their climate neutrality, efficiency, technological maturity for fossil–fuel substitution or supplement and their role in the European energy system.

Lai, et al. [18] conducted a study on strategies to increase energy savings while decreasing coal consumption through optimisation models applied to parallel CHP units which are connected to a heat storage tank (or TES). Using a similar setup of CHP units and buffer tank, Wang, et al. [19] introduced a buffer tank capacity configuration method for a CHP plant to improve peak shaving ability.

Apart from Maruf, et al. [17], Lai, et al. [18] and Wang, et al. [19], who provided holistic energy solutions and insights to CHP systems, the studies mentioned before focussed more on TES devices and provided useful insights and methods for analysing and characterising thermal stratification. The most notable factors influencing stratification were the inlet water temperature, its flow rate and the set/target temperature of the device thermostat. The flow rate of the incoming water has a direct influence on the degree of turbulence of the inlet water stream. A higher flow rate would cause a higher degree of turbulence, as per the Reynolds number, and thus induce more mixing in the tank [9,10,14,16]. This ultimately decreases the exergy in the system as entropy increases due to thermal diffusion. For this purpose, low flow rates are favourable when the quality of thermal stratification needs to be maximised. Other notable studies include Kizilors, et al. [20], Farooq, et al. [21], Abdelhak, et al. [22], and Chandra, et al. [23].

Most studies from literature that focus on thermal stratification, including the studies discussed above, use conventional TES tanks with plumbing configurations fitted with single inlet and single outlet ports. However, TES buffer tanks that are utilised in cogeneration applications are fitted with two or three pairs of inlet-outlet ports, as shown in Figs. 2 and 3. Table 1 provides a visual comparison between studies mentioned above and highlights the relevant research gaps that this paper aims to address.

One notable difference between the above-mentioned studies is the thermal charging mechanisms for heating operations. Most studies focus on resistive heating, whereas TES tanks in cogeneration applications are charged by circulation; replacing cold water with heated water directly from a CHP unit's heat exchanger. From this, two significant differences are identified between conventional TES tanks and TES buffer tanks that are utilised in cogeneration applications — port configurations and heating mechanism.

Table 1 shows the scarcity of literature examining the impact of thermal stratification on the overall efficiency of TES buffer tanks installed in CHP configurations. Conventional characterisation strategies from existing literature will be applied to the thermodynamic data from the buffer tank used in a cogeneration application. The aim will be to test whether these stratification characterisation strategies are applicable to TES tanks with cogeneration configurations. Furthermore, if they are, another remaining question would be if they can be used to characterise the TES device's thermodynamic effectiveness appropriately.

3. Experimental setup

Fig. 1 shows the high-level experimental setup. It consists of a CHP unit "Dachs G5.5" by SenerTec driven by natural gas providing 5.3 kW net electric and 12.0 kW thermal power. The TES is the SenerTec SE 750, made by SenerTec as well, with an internal volume of 750 litres.

The hydraulics and the instrumentation of the test bench are illustrated in Fig. 2. The thermal energy storage is shown in the centre of the diagram, with the CHP unit on the left and circuits for domestic hot water (DHW) and space heating forming the demand side on the right.

It can be seen that the TES is charged by the CHP unit, which operates in On/Off-mode, by feeding hot water in the supply line to the tank. For discharging, thermal energy is transferred to a heat exchanger for generation of DHW and to a circuit for space heating. The two-way control valves in the fresh water circuits are meant for maintaining a predefined heat demand for DHW and space heating, respectively. In addition, a three-way control valve is installed in the circuit for feeding the heat exchanger for space heating with a constant and pre-defined supply temperature. By this means, any profile for DHW as well as heating load can be applied.

However, for reducing the number of input parameters and facilitating the analysis of the tests in the course of this paper, only the heating circuit was utilised to discharge the TES. The circuit for DHW was not in operation during the tests. Moreover, it can be seen from Fig. 2 that numerous sensors for temperatures and volume flow rates were installed, in order to evaluate heat rates as well as temperature distribution in the TES. For the latter, seven thermocouple sensors of type K were attached by high-conductivity glue on the outside of the tank (TC1-7). Sensors TC1-7 were intended to be placed evenly distributed over the height of the tank, which, however, was not entirely possible due to the fact that a commercially tank was applied.

To increase the accuracy of the measurements, the thermocouple sensors were calibrated against each other at ambient temperature, which was adequate because the temperature differences to this reference is of interest for the further analysis, only. Temperatures T_{upper}, T_{middle} and T_{lower} were measured by standard Pt500 sensors. All other temperature sensors depicted in Fig. 2 were Pt100 type B 1/10 DIN allowing, together with the magnetic-inductive volume flow meters, relative uncertainties below 1.5 % for the heat rates for charging and discharging the TES.

During the experiments the CHP unit operated in heat-led mode, whereby it turned on whenever the status of the TES was "fully discharged" and continued in this state until the status of the TES turned to "fully charged". From that point onward the CHP unit stayed off, and the heat demand was covered by the TES only. This state remained operational until the TES was fully discharged, forcing the CHP unit to be turned on again, and the cycle to start anew.

Turning the status of the TES from "fully discharged" to "fully charged" or the other way around is determined and executed by the three temperature sensors attached to the TES tank T_{upper}, T_{middle} and T_{lower}, shown in Fig. 2. For this purpose, these sensors are typically directly connected to the internal control of the CHP unit. In the event

Table 1
Comparative summary of relevant stratification literature.

Study	Stratification indices[a]	Measurements[b]	TES and CHP combination	Stratification modelling	Controlled parameter variation	Exergy analyses	TES heating method
[11]	✓	✓(11)	✗	✗	✓	✓	Resistive
[21]	✗	✓(8)	✗	✓(FEA)	✗	✗	Resistive
[22]	✓	✓(data [11])	✗	✓(CFD)	✗	✗	Resistive
[24]	✗	✓(11)	✗	✓(Multiple)	✓	✗	Resistive
[20]	✗	✓(33)	✗	✗	✓	✗	Resistive
[10]	✗	✓(12)	✗	✓(VTC,CFD)	✓	✗	Circulation
[23]	✓	✓(20)	✗	✓(CFD)	✓	✗	Circulation
[13]	✓	✓(6)	✗	✗	✓	✗	Circulation
[15]	✗	✗	✗	✓(TRNSYS)	✗	✓	Circulation
[16]	✓[c]	✓(16)	✗[d]	✓(CFD)	✓	✓	Circulation
[18]	✗	✗	✓	✗	✗	✓	Circulation
This study	✓	✓	✓	✗	✓	✓	Circulation

[a]Note that all TES tanks are oriented vertically in these studies.
[b]The measurements column includes the number of sensors used for stratification measurement in brackets.
[c]Definition of new stratification performance index - fill efficiency.
[d]Solar setup - TES plumbing configuration very similar

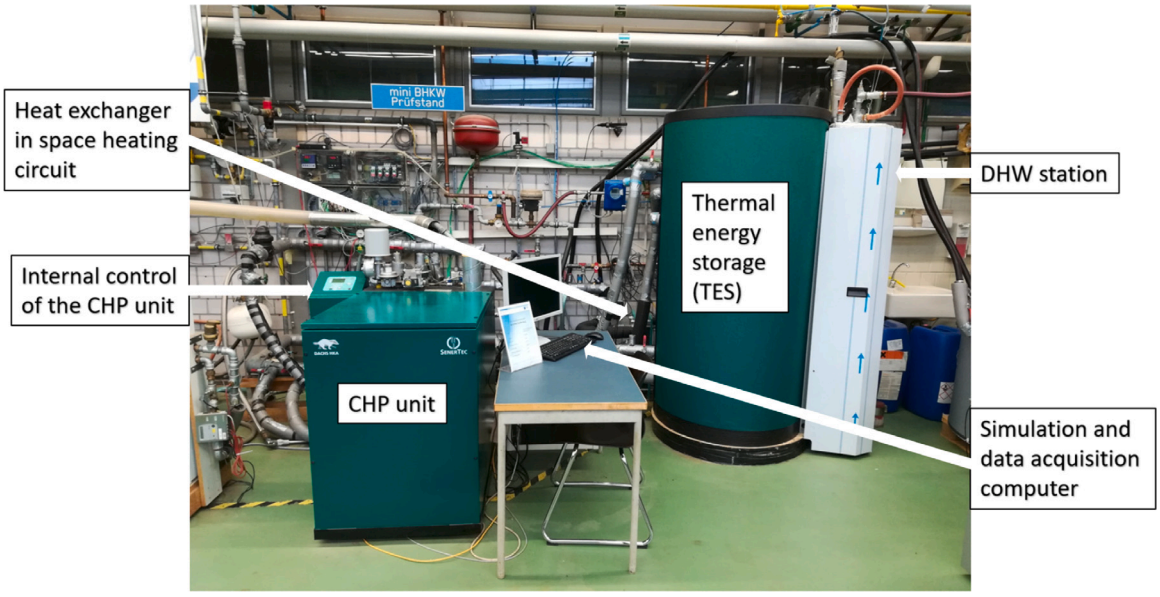

Fig. 1. Test bench setup at Reutlingen University.

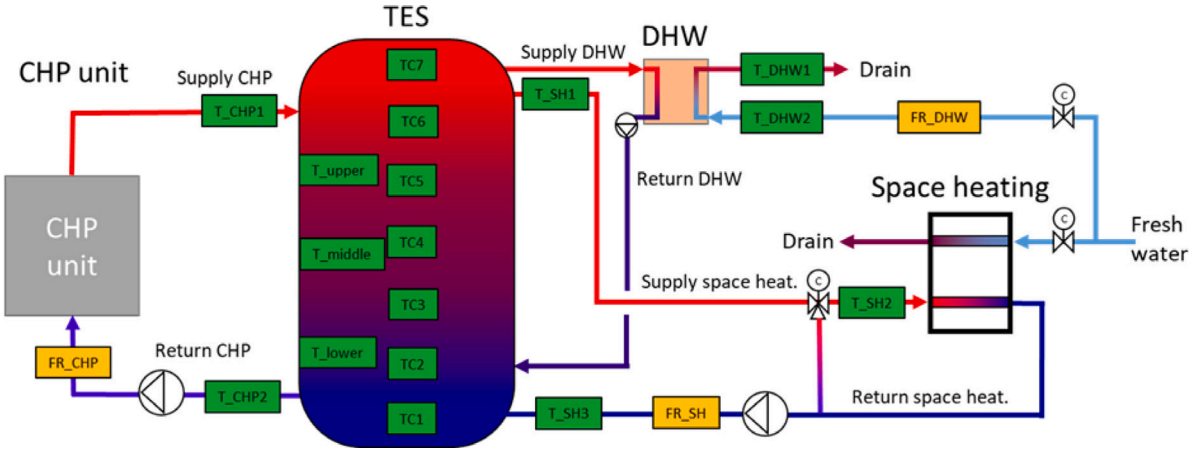

Fig. 2. Schematic view of the test bench (T: temperature sensor, FR: volume flow meter, C: control valve).

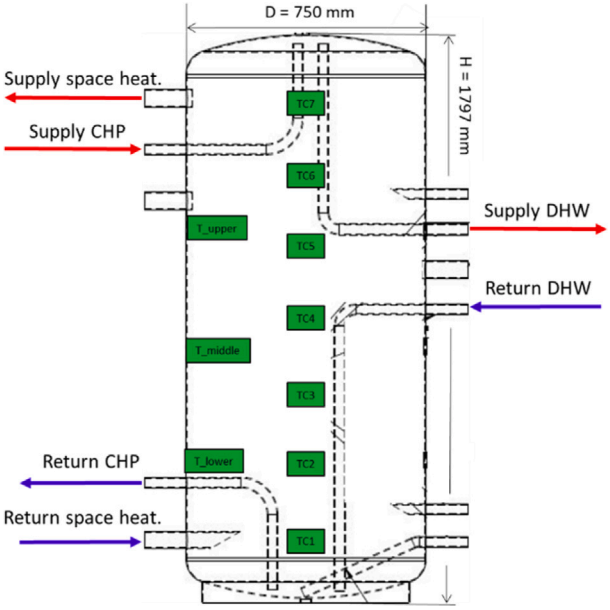

Fig. 3. Details of the TES at the test station.

of the temperature at the upper sensor dropping below a predefined set point temperature, the TES is termed discharged, and the status of the TES is set to "fully discharged" by the internal control forcing the CHP unit to turn on, as described before.

On the other hand, whenever the temperature at the lower sensor exceeds its predefined set point temperature, the TES status is turned to "fully charged", and the CHP unit turns off. This description implies that only two of the three sensors shown in Fig. 2 are needed to control the CHP unit in heat-led mode. However, the third sensor placed in the middle of the tank is used to replace either the lower or the upper sensor for different control modes such as comfort or energy saving mode. The latter mode operates the CHP unit only between the middle and the upper sensor providing that the lower section of the TES always stays cold, which tends to reduce heat losses from the TES. This mode is often applied in summer time, when heat is needed for generation of DHW, only. In comfort mode the CHP unit operates between the lower and the middle sensor making a bigger portion of hot water available in the top of the tank, which can i.e. be used for generating more DHW.

Fig. 3 shows a more detailed sketch of the TES, revealing the positions of the sensors $TC1$–$TC7$ as well as T_{upper}, T_{middle} and T_{lower} more exactly. In addition, the locations of the connecting pipes for the different circuits are visible. Any further nozzles depicted in Fig. 3 were plugged. It should be noted that the connecting pipes may be extended internally, in order to direct their inlets or outlets directly to the top or the bottom of the tank. By this means, it is guaranteed that i.e. the hottest section in the top of the tank is utilised for DHW generation and the CHP unit is provided from the coldest section at the bottom of the tank for maximising heat recovery from the exhaust gases including condensation. Moreover, it should be noted that the fluids of the CHP circuit, DHW and space heating circuit can mix within the tank. Hence, there is no separation of the fluids by an internal heat exchanger, which saves cost and is for that reason typical for most CHP installations. As a consequence, thermal stratification may occur over the entire height of the tank.

To facilitate the analysis of the TES, its geometry featuring the two torispherical heads has been converted to an ideal cylinder with a constant volume of 750 litres and a constant internal diameter of 0.744 m. Hence, the height of the ideal cylinder is reduced from 1.823 m to 1.725 m. In the same way the heights of the different sensor locations, each measured from the bottom of the tank, have been converted to the ideal cylinder. Table 2 lists these heights as dimensionless relative heights based on the total height of the theoretical cylinder. In addition, each sensor is related to its partial volume, which is represented by the volume slice resulting from cutting the total volume at half the distance between two neighbouring sensor positions. This method was performed independently for sensors $TC1$–$TC7$ and for sensors T_{lower}, T_{middle} and T_{upper}, and the results are listed in Table 2 as dimensionless relative partial volumes based on the total volume of the tank, which is 750 litres.

As outlined before, it was intended to space the sensors equally along the height of the tank, in order to create almost identical partial volumes for each section. Due to the fact that a commercially available tank was applied, this was not entirely possible. But the remaining variations between the partial volumes does not affect the general conclusions of the analysis.

4. Performance indices

There are many theoretical and practical methods that can be used to quantify the performance and efficiency of thermal energy storages such as the one investigated in this paper and described in the previous section. In addition, many resources, strategies and numbers exist in literature to analyse the quality of thermal stratification in hot water tanks as summarised in Section 2. This section provides a detailed overview of a few numerical indicators that were used to quantify the thermal performance of the tank for the different experiments as outlined before.

4.1. TES content of energy

For an adequate analysis of thermal stratification in a TES the tank needs to be divided in a number of J layers, with every layer being equipped with a temperature sensor. In the experimental setup, the tank was divided into seven layers as discussed in Section 3. The internal energy for each layer can thus be determined based on each layer's measured temperature and pre-defined volume; the latter as listed in Table 2. As one metric of interest is the total internal energy inside the tank, it can simply been derived from the sum of the internal energy for each measured layer. This is expressed as

$$E_{\text{TES}}(t) = \sum_{j=1}^{J} \rho_j(T_j(t)) \cdot c_{p,j}(T_j(t)) \cdot V_j \cdot (T_j(t) - T_{\text{ref}}) \tag{1}$$

where E_{TES} is the internal energy of the thermal energy storage, as a function of time and measured in Joule. The variables ρ_j, $c_{p,j}$ and T_j are the density, specific heat, and measured temperature of the water in the j'th layer, respectively. The variables V_j and T_{ref} are the predefined volume of the j'th layer and the reference temperature for all layers, respectively. All calculations in this paper assume a reference temperature of 20 °C. Finally, index J is 7 with respect to the tank under investigation.

The mixed (bulk mean) temperature, T_{m} is used in many cases where the weighted average temperature is needed. It is expressed as

$$T_{\text{m}}(t) = \frac{1}{V_{\text{tank}}} \cdot \sum_{j=1}^{J} V_j \cdot T_j(t) \tag{2}$$

where V_{tank} is the total tank volume of in this case 750 litres. Density and specific heat properties are treated as constants in this equation, in order to prevent an iterative process for finding $T_{\text{m}}(t)$. The resulting error is small as long as temperatures in the tank do not differ too much from one another.

Table 2
Relative heights of sensor locations for the ideal cylindrical tank and relative partial volumes.

Sensor	TC1	TC2	TC3	TC4	TC5	TC6	TC7	T_{lower}	T_{middle}	T_{upper}
Rel. height/-	0.081	0.224	0.343	0.467	0.605	0.747	0.909	0.177	0.458	0.781
Rel. part. volume/-	0.163	0.122	0.116	0.133	0.142	0.142	0.182	0.354	0.209	0.437

4.2. TES effective capacity

The effective capacity of the TES can be defined as the difference between the maximum content of internal energy to the minimum content of internal energy in time. According to Section 3, the maximum content of internal energy occurs whenever the TES reaches the status "fully charged", while the minimum content of internal energy occurs when the TES reaches the status "fully discharged". Hence, the effective capacity $Q_{\mathrm{TES,eff}}$ can be expressed by the following equation:

$$Q_{\mathrm{TES,eff}} = E_{\mathrm{TES,max}} - E_{\mathrm{TES,min}} \tag{3}$$

It is important to note that $Q_{\mathrm{TES,eff}}$ is not a function of time anymore from when the quasi-steady state of the TES is reached, as $E_{\mathrm{TES,max}}$ refers to the energy at the time instant when the TES is fully charged, which is equivalent to the time when the CHP unit is turned off by the internal control. Consequently, the TES reaches its minimum content of internal energy $E_{\mathrm{TES,min}}$ at times where it is fully discharged, which is the time where the CHP unit is turned on.

4.3. Stratification indices

Thermal stratification is a natural phenomena that occurs due to fluid density differences. Naturally, a fluid having a lower density would rise, and remain above a fluid with a higher density. The density of any liquid has an inversely proportional relationship with temperature. That being said, an increase in temperature for a body of water would mean a decrease in density for that same body of water. In a common case where a region of water within the lower region of a water tank is heated, the water molecules in this region would start to rise to the top, and accumulate. This buoyancy effect is the reason why thermal stratification occurs. It is a common phenomena and also an indication of the amount of usable energy, also known as exergy, within the TES tank. The degree of stratification and exergy can be analysed in various ways — many of which are explained in the following sections.

In order to support these explanations, Fig. 4 illustrates the definition of various parameter used in the following for deriving the metrics. In addition, besides the experimental case displayed in the middle of Fig. 4 two reference cases are shown. The first case on the left represents a theoretical case of an ideally-stratified tank with two volumes — a hot epilimnion and a cold hypolimnion. Note that these volumes are dynamic and vary as a function of time. The tank presented in the middle represents the experimental case where the tank is sectioned, and temperatures measured at seven different locations along the height of the TES tank. For the sake of simplicity the sections are displayed with equal volumes, which could not be met entirely for the tank applied, as explained in conjunction with Table 2. The third case, as seen on the right, represents the theoretically isothermal tank having only a single volume showing no stratification at all.

4.3.1. Stratification number (Str)

The stratification number is defined as the ratio of the average temperature gradients at any time for thermal charging or discharging to that of the maximum average temperature gradient in a TES tank, the latter referring to ideal thermal stratification. This non-dimensional evaluation metric is used and discussed in Fernández-Seara, et al. [25], Abdelhak, et al. [26] and Chandra, et al. [12]. The number is defined as

$$Str(t) = \frac{\overline{\left(\frac{\partial T}{\partial z}\right)_t}}{\overline{\left(\frac{\partial T}{\partial z}\right)_{\max}}} \tag{4}$$

$$\overline{\left(\frac{\partial T}{\partial z}\right)_t} = \frac{1}{J-1} \cdot \sum_{j=1}^{J-1} \left(\frac{T_{j+1} - T_j}{\Delta z}\right) \tag{5}$$

$$\overline{\left(\frac{\partial T}{\partial z}\right)_{\max}} = \frac{T_{\max} - T_{\mathrm{in,cold}}}{(J-1)\Delta z} \tag{6}$$

where J is the number of vertical layers, Δz is the vertical distance between the centre points of the layers and T_j is the measured temperature at layer number j. The variable $T_{\max}$ represents the maximum measured temperature in the time series data set for all layers (or a pre-defined hot reference temperature) and $T_{\mathrm{in,cold}}$ is the temperature of the cold water entering the tank.

However, in order to characterise stratification in a vertical tank, especially with equally spaced temperature sensors along its height, stratification number is not an adequate criterion for the following reason: Given the case of equally spaced temperature sensors, the variable Δz becomes constant, and Eq. (5) reduces to:

$$\overline{\left(\frac{\partial T}{\partial z}\right)_t} = \frac{T_{\mathrm{top}}(t) - T_{\mathrm{bot}}(t)}{(J-1)\cdot\Delta z} \tag{7}$$

It can be seen that only the temperatures in the top and the bottom layer remain in the equation while all temperatures of the intermediate layers cancel out. For that reason the information about temperature distribution along the height of the tank is no longer included in stratification number. Moreover, using $T_{\mathrm{top}}(t)$ and $T_{\mathrm{bot}}(t)$ to represent $T_{\max}$ and $T_{\mathrm{in,cold}}$ as reference temperatures for ideal stratification in Eq. (6), the stratification number will reduce just to a constant value of 1.

4.3.2. Stratification factor (ST)

The stratification factor, also known as the stratification coefficient, was first defined by Wu and Bannerot [27]. The number represents the mass weighted mean square deviation of the temperatures in the different layers from a theoretically-defined uniformly mixed temperature, T_{m} [12]. It is similar to the Stratification number as it does not show any indication of the influence of mixing forces on thermal stratification or the content of energy stored. It purely focuses on temperature gradients. This makes it a good gauge for the temperature deviation profiles from a reference of a perfectly isothermal tank at temperature T_{m} [12]. The number is defined as

$$ST(t) = \frac{1}{m_{\mathrm{storage}}} \cdot \sum_{j=1}^{J} m_j \cdot [T_j(t) - T_{\mathrm{m}}(t)]^2 \tag{8}$$

$$ST(t) = \frac{1}{\rho(T_{\mathrm{m}}(t)) \cdot V_{\mathrm{tank}}} \cdot \sum_{j=1}^{J} [\rho_j(t) \cdot V_j \cdot [T_j(t) - T_{\mathrm{m}}(t)]^2] \tag{9}$$

where T_j and V_j are the temperature and the layer volume at measurement node j. The parameter T_{m} is the bulk mean temperature as defined in Eq. (2).

Note that to the authors' knowledge the stratification factor has not been defined to be dimensionless in literature. However, it would be beneficial to transform this number into a dimensionless number so that it could be compared to and represented on the same scale as other numbers. For this reason stratification factor has been derived for an ideally-stratified tank as a reference. According to Fig. 4 Eq. (9) transforms as follows:

$$ST_{\mathrm{ideal\text{-}str}}(t) = \frac{1}{\rho(T_{\mathrm{m}}(t)) \cdot V_{\mathrm{tank}}} \cdot [\rho(T_{\mathrm{top}}(t)) \cdot V_{\mathrm{hot}}(t) \cdot [T_{\mathrm{top}}(t) - T_{\mathrm{m}}(t)]^2 + \rho(T_{\mathrm{bot}}(t)) \cdot V_{\mathrm{cold}}(t) \cdot [T_{\mathrm{bot}}(t) - T_{\mathrm{m}}(t)]^2] \tag{10}$$

If, for the sake of simplicity, the variation of density with temperature is neglected, this term cancels out in Eq. (10). Introducing

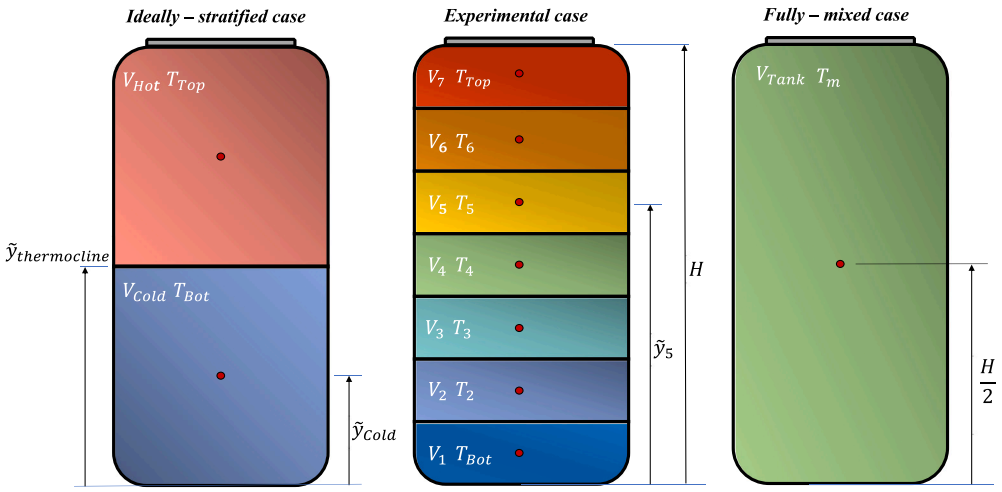

Fig. 4. Principle of an ideally-stratified tank (left), the experimental tank (middle) and a fully-mixed tank (right).

furthermore bulk mean temperature T_m as the average of T_top and T_bot the volumes cancel out as well and the equation for the stratification factor in case of an ideally-stratified tank reduces to

$$ST_\mathrm{ideal\text{-}str}(t) = \left(\frac{T_\mathrm{top}(t) - T_\mathrm{bot}(t)}{2}\right)^2 \tag{11}$$

where T_top and T_bot are the temperatures in the top and bottom layer, respectively. Essentially, the reference term is the square of half of the difference between the temperature of the hottest layer at the top of the tank and the lowest temperature at the bottom. Compared to the definition of stratification factor as a mass weighted average according to Eq. (8) the reference does not consider the masses of the hot and the cold volumes. At first glance, this might seem to be a major simplification. But, taking in mind that it only affects the reference, it should become clear that the information about the temperature distribution in the tank, which enters the stratification factor through Eq. (9) is not affected at all. Thus, the following equation defines the normalised stratification factor, which is denoted as ST^*:

$$ST^*(t) = \frac{ST(t)}{ST_\mathrm{ideal\text{-}str}(t)} \tag{12}$$

Moreover, for the same reason ideal stratification should be represented by a value of 1, while a fully mixed tank should a result in a value for the metric of 0.

4.3.3. Peclet number (Pe)

The Peclet number is defined as the ratio of the rate of mass and energy transport by fluid flow to the rate of thermal diffusion of the same quantity of fluid driven by the temperature gradient in the tank. In other words, it provides a relationship between conductive heat transfer and bulk heat transfer in the water. A large Peclet number would visually represent a thin thermocline whereas the converse is true for smaller Peclet numbers. This concept is illustrated in Chandra et al. [12] who further state that higher Peclet numbers imply lower values of diffusivity and lower rates of thermocline decay. The equation for the Peclet number is

$$Pe(t) = \frac{\upsilon(t) \cdot H}{\alpha(T_\mathrm{m}(t))} \tag{13}$$

$$\upsilon(t) = \frac{\dot{V}(t)}{\pi \cdot D^2} \tag{14}$$

where H and D are the height and internal diameter of the tank, α is the thermal diffusivity of the fluid evaluated at the bulk mean temperature and $\dot{V}$ is the discharge rate in m^3/s. The discharge rate causes difficulties in applying the Peclet number for water tanks serving as TES in a CHP installation, because there are two flow rates involved, one in the discharge line and one in the charging line. One may argue that the net flow rate in the tank can serve as an appropriate measure in this respect, but this term will become positive as well as negative depending on the dominant flow rate. When charging the TES, the net flow in the tank is directed from top to bottom. During discharging the direction of flow is opposite. In addition, the net flow rate varies discontinuously with time due to the On/Off-operation of the CHP unit. Both effects disqualify the Peclet number as a metric for proper interpretation of stratification in this application.

4.3.4. Richardson number (Ri)

The Richardson number characterises the ratio between the potential energy required for vertical mixing and the turbulent energy required for such a process. The Richardson number is defined as

$$Ri(t) = \frac{g \cdot \beta \cdot H \cdot (T_\mathrm{top}(t) - T_\mathrm{bot}(t))}{\upsilon(t)^2} \tag{15}$$

where $\upsilon(t)$ is defined by Eq. (14), g is the gravitational acceleration constant and β is the coefficient of thermal expansion. A small Richardson number indicates a relatively mixed or thermally unified tank whereas a larger number indicates a stratified tank. This number is a good measure of thermal stratification as it takes into account the overall working temperature and flow rate. According to [13], the Richardson number in combination with the Peclet number is very useful for characterising thermal stratification. However, in applications with two opposed and discontinuous flow rates as given in CHP installations, the Richardson number is not appropriate for the same reasons as the Peclet number, since it also depends on fluid flow rate $\dot{V}$.

4.3.5. MIX number

The MIX number is extensively discussed in Castell, et al. [13] and Chandra, et al. [12]. As opposed to the stratification number (Str) that mainly focuses on the temperature profiles and temperature deviations of the tank, the MIX number considers the total energy stored in the tank for each time step in addition to vertical energy variation, which depends on the vertical distribution of temperatures in the tank. It is determined by evaluating the first moment of energy (M_E) which considers energy location. This method is also used and discussed in Wang et al. [16] for a similar setup. The internal energy at each measured node is summed and weighted according to the height of its location [12]. The MIX number is defined as

$$\mathrm{MIX}(t) = \frac{M_{E,\mathrm{ideal\text{-}str}}(t) - M_{E,\mathrm{exp}}(t)}{M_{E,\mathrm{ideal\text{-}str}}(t) - M_{E,\mathrm{fully\text{-}mixed}}(t)} \tag{16}$$

The $M_{E,\mathrm{exp}}$ and $M_{E,\mathrm{fully\text{-}mixed}}$ terms represent the experimentally-measured moments of energy in the tank based on the temperature

$$V_{\text{hot}}(t) = \frac{E_{\text{exp}}(t) - \rho(T_{\text{bot}}(t)) \cdot c_p(T_{\text{top}}(t)) \cdot V_{\text{tank}} \cdot (T_{\text{bot}}(t) - T_{\text{ref}})}{\rho(T_{\text{top}}(t)) \cdot c_p(T_{\text{top}}(t)) \cdot (T_{\text{top}}(t) - T_{\text{ref}}) - \rho(T_{\text{bot}}(t)) \cdot c_p(T_{\text{bot}}(t)) \cdot (T_{\text{bot}}(t) - T_{\text{ref}})} \tag{24}$$

Box I.

at different layers and the moment of energy for a thermally-uniform tank, respectively. Obviously, the latter is based on the mean bulk temperature as given by Eq. (2),

$$M_{E,\text{exp}}(t) = \sum_{j=1}^{J} \tilde{y}_j \cdot E_j(t) = \sum_{j=1}^{J} \left[\tilde{y}_j \cdot \left[\rho(T_j(t)) \cdot c_p(T_j(t)) \cdot V_j \cdot (T_j(t) - T_{\text{ref}})\right]\right] \tag{17}$$

$$M_{E,\text{fully-mixed}}(t) = \frac{H}{2} \cdot \left[\rho(T_m(t)) \cdot c_p(T_m(t)) \cdot V_{tank} \cdot (T_m(t) - T_{\text{ref}})\right] \tag{18}$$

Note that $\tilde{y}_j$ is the distance measured from the bottom of the tank to the centre point of layer j, while for the fully mixed tank this distance simply comes to half of the total height H of the tank (see Fig. 4).

The term $M_{E,\text{ideal-str}}$ is calculated as shown in Eq. (19) and represents the moment of energy for a ideally-stratified tank that theoretically consists of only two thermally-separated volumes, V_{hot} and V_{cold}.

$$M_{E,\text{ideal-str}} = \tilde{y}_{\text{cold}}(t) \cdot E_{\text{cold}}(t) + \tilde{y}_{\text{hot}} \cdot E_{\text{hot}}(t) \tag{19}$$

While the $\tilde{y}_j$ terms are predefined constants when calculating $M_{E,\text{exp}}$, the corresponding distances $\tilde{y}_{\text{hot}}$ and $\tilde{y}_{\text{cold}}$ for calculating $M_{E,\text{ideal-str}}$ vary as a function of time. This is because the calculation of the hot and cold volumes change in time based on internal energy changes. From the energy balance of the ideally stratified tank

$$E_{\text{ideal-str}}(t) = E_{\text{exp}}(t) = E_{\text{cold}}(t) + E_{\text{hot}}(t) \tag{20}$$

using

$$E_{\text{cold}}(t) = \rho(T_{\text{bot}}(t)) \cdot c_p(T_{\text{bot}}(t)) \cdot V_{\text{cold}}(t) \cdot (T_{\text{bot}}(t) - T_{\text{ref}}) \tag{21}$$

$$E_{\text{hot}}(t) = \rho(T_{\text{top}}(t)) \cdot c_p(T_{\text{top}}(t)) \cdot V_{\text{hot}}(t) \cdot (T_{\text{top}}(t) - T_{\text{ref}}) \tag{22}$$

and

$$V_{\text{tank}} = V_{\text{cold}}(t) + V_{\text{hot}}(t) \tag{23}$$

the equation for the hot volume as a function of time reads as follows in Box I:

From Eq. (24) can be seen that the temperature in the cold volume relates to the temperature in the bottom of the tank $T_{\text{bot}}(t)$, which refers to the measured temperature in the bottom layer $T_1(t)$, as illustrated in Fig. 4. Similarly, the temperature in the top of the tank $T_{\text{top}}(t)$ refers to the measured temperature in the top layer $T_7(t)$. With $V_{\text{cold}}(t)$ from Eq. (23) the distances $\tilde{y}_{\text{hot}}$ and $\tilde{y}_{\text{cold}}$ can be expressed by the following equations:

$$\tilde{y}_{\text{cold}}(t) = \frac{2 \cdot V_{\text{cold}}(t)}{\pi D^2} \tag{25}$$

$$\tilde{y}_{\text{hot}}(t) = y_{\text{thermocline}}(t) + \frac{2 \cdot V_{\text{hot}}(t)}{\pi \cdot D^2} = \frac{2 \cdot (2 \cdot V_{\text{cold}}(t) + V_{\text{hot}}(t))}{\pi \cdot D^2} \tag{26}$$

where $y_{\text{thermocline}}(t)$ is the theoretical vertical distance to the location of the thermocline, as measured from the bottom of the tank (see Fig. 4), and D is the internal diameter of the tank, which is treated as an ideal cylinder.

Finally, a modification was implemented, because the MIX number intuitively represents the inverse effect of thermal stratification — which is mixing. Since most of the other performance metrics evaluate on the basis of stratification, it is useful to modify the MIX number so that it could be represented on the same scale as the other metrics between 1 for the ideally-stratified case and 0 for the fully-mixed case. The modified MIX number is denoted as MIX* and is expressed as

$$\text{MIX}^*(t) = 1 - \text{MIX}(t) = \frac{M_{E,\text{exp}}(t) - M_{E,\text{fully-mixed}}(t)}{M_{E,\text{ideal-str}}(t) - M_{E,\text{fully-mixed}}(t)} \tag{27}$$

4.4. Exergy analyses

Exergy is a thermodynamic measure of how much useful energy is available within a given system and can thus be extracted from the system before it reaches a state of equilibrium with its environment. In contrast to energy analyses, exergy is not conserved. Instead, it is reduced by systemic irreversibilities. For that reason, it is helpful from a thermodynamic point of view to investigate the content of exergy in a system as it presents a practical and relatable result to what is expected in practical operation with respect to irreversible processes like destruction of thermal stratification in a TES.

4.4.1. Exergy number (Ex^*)

As discussed before, the MIX* number provides a useful approach to evaluate thermal stratification of the TES. It would therefore also be useful to apply the MIX* number equations to the exergy of the tank in the same three states, namely "ideal-stratified", "experimentally measured" and "fully-mixed" as introduced in Fig. 4. Hence, similarly to the MIX* number in Eq. (27), the exergy number Ex^* is defined as

$$Ex^*(t) = \frac{Ex_{\text{exp}}(t) - Ex_{\text{fully-mixed}}(t)}{Ex_{\text{ideal-str}}(t) - Ex_{\text{fully-mixed}}(t)} \tag{28}$$

where $Ex_{\text{exp}}(t)$ represents the total exergy content of the TES for the actual experimental case and is accumulated from each layer as follows

$$Ex_{\text{exp}}(t) = \sum_{j=1}^{J} \rho_j(T_j(t)) \cdot c_{p,j}(T_j(t)) \cdot V_j \cdot \left((T_j(t) - T_{\text{ref}}) - T_{\text{ref}} \cdot \ln\left(\frac{T_j(t)}{T_{\text{ref}}}\right)\right) \tag{29}$$

where T_{ref} is the reference temperature as discussed in Section 4.1. Properties $\rho_j(T_j(t))$ and $c_{p,j}(T_j(t))$ are the density and the specific heat capacity of the fluid at layer j, evaluated at the measured layer temperature, T_j.

The parameters $Ex_{\text{fully-mixed}}$ and $Ex_{\text{ideal-str}}$ represent the two theoretically obtained boundary cases — the total exergy content for a fully-mixed tank and for a ideally-stratified tank, respectively. $Ex_{fully-mixed}$ is expressed by

$$Ex_{\text{fully-mixed}}(t) = \rho(T_{\text{m}}(t)) \cdot c_p(T_{\text{m}}(t)) \cdot V_{\text{tank}} \cdot \left((T_{\text{m}}(t) - T_{\text{ref}}) - T_{\text{ref}} \cdot \ln\left(\frac{T_{\text{m}}(t)}{T_{\text{ref}}}\right)\right) \tag{30}$$

where properties $\rho(T_{\text{m}}(t))$ and $c_p(T_{\text{m}}(t))$ represent density and specific heat of the fluid at bulk mean temperature $T_{\text{m}}(t)$ as expressed in Eq. (2).

According to Fig. 4, the exergy content of the ideally-stratified TES again assumes a hot volume in the top of the tank and a cold volume below. In this case, the total exergy is the sum of exergies of the two volumes, while the exergy of each of the two volumes can be derived as expressed by Eqs. (32) and (33).

$$Ex_{\text{ideal-str}}(t) = Ex_{\text{cold}}(t) + Ex_{\text{hot}}(t) \tag{31}$$

$$Ex_{\text{cold}}(t) = \rho(T_{\text{bot}}(t)) \cdot c_p(T_{\text{bot}}(t)) \cdot V_{\text{cold}}(t) \cdot \left((T_{\text{bot}}(t) - T_{\text{ref}}) - T_{\text{ref}} \cdot \ln\left(\frac{T_{\text{bot}}(t)}{T_{\text{ref}}} \right) \right) \quad (32)$$

$$Ex_{\text{hot}}(t) = \rho(T_{\text{top}}(t)) \cdot c_p(T_{\text{top}}(t)) \cdot V_{\text{hot}}(t) \cdot \left((T_{\text{top}}(t) - T_{\text{ref}}) - T_{\text{ref}} \cdot \ln\left(\frac{T_{\text{top}}(t)}{T_{\text{ref}}} \right) \right) \quad (33)$$

The definitions of the volumes V_{cold} and V_{hot} are applied as derived for the momentum of energy of an ideal stratified tank $M_{E,\text{ideal-str}}$; hence they are calculated as given by Eqs. (23) and (24). Similarly, the temperature of the cold volume refers to the measured temperature of the bottom layer $T_{\text{bot}}(t)$, whereas the temperature of the hot volume refers to the temperature of the top layer $T_{\text{top}}(t)$. Finally, it should be noted that exergy number Ex^* ranges in analogy to MIX* number from 1 for an ideally-stratified tank to 0 for a fully-mixed tank.

4.4.2. Exergy efficiency (η_{Ex})

Another useful metric to be used as a comparative number is the exergy efficiency of the TES, defined as the ratio between the actual experimental exergy $Ex_{\text{exp}}(t)$ and the theoretically best case of the exergy for an ideally-stratified tank $Ex_{\text{ideal-str}}(t)$. Accordingly, exergy efficiency is expressed as

$$\eta_{\text{Ex}}(t) = \frac{Ex_{\text{exp}}(t)}{Ex_{\text{ideal-str}}(t)} \quad (34)$$

For an ideally-stratified tank exergy efficiency reaches a maximum value of 1. In contrast to the two metrics discussed before, a fully mixed tank is not represented by an exergy efficiency of 0. Instead, it is a value higher than 0 but smaller as 1.

4.5. Short discussion

A variety of performance and evaluation metrics have been discussed in this chapter — all of which collectively aim to evaluate the thermodynamic performance of the TES. However, based on the analyses, it is clear that some metrics are more suited than others for evaluation of thermal stratification in a TES as part of a CHP installation. The one significant difference between such a TES and, for example, an electrically heated hot water tank for domestic hot water (DHW) generation, is the number of inlet and outlet ports. While the DHW tank has only one inlet and one outlet port; in a CHP installation there are additional ports for hot water inlet and outlet from and to the CHP unit. This evidently affects the flow regime in the tank and therefore the temperature distribution and thermal stratification. Since most of the metrics were derived for one inlet and one outlet port, they cannot cope with additional ports as outlined above when discussing the Peclet and Richardson number. Both numbers are well-known from other fields, and they may be modified or expanded for a TES in combination with a CHP unit, but this was not within the scope of this work. For that reason, the Peclet number and Richardson number will not be considered in the rest of this paper. Moreover, the stratification number will also not be included in the further analysis, because the effect of the temperature distribution in the tank cancels out, as outlined above. Nevertheless, this metric is still useful for electrically heated hot water tanks, for which it was originally designated. As a result, besides the effective capacity of the TES, the metrics normalised stratification factor ST^*, modified MIX number MIX*, exergy number EX^* and exergy efficiency η_{Ex} will be used in the rest of the paper for analysing the effect of thermal stratification in the TES and on its performance in CHP installations.

5. Experimental procedure

In view of the relevance for practical applications as well as against the background of the implementation at the test rig, the following three parameters were selected to analyse their influence on thermal stratification in a thermal energy storage.

- A: Thermal load
- B: Thermal load profile
- C: Sensor position

To analyse the effect of each parameter and their combinations, the technique of Design of Experiments (DoE) was used, and consequently each parameter was set to a minimum and a maximum value. Adapted to the thermal power of the CHP unit of 12 kW, the thermal load (parameter A) is set to a minimum value of 3 kW and a maximum value of 8 kW. Parameter B describes the profile of the thermal load. In “constant” mode the thermal energy storage is constantly discharged with the thermal load defined via parameter A. With the setting “variable”, on the other hand, an hourly variable load profile is applied, which is based on a consumption profile of a typical single-family household. In this case, the load profile is scaled in a way that on average the thermal load defined via parameter A is obtained. Thereby, the same amount of energy of either 72 kWh (at a thermal load of 3 kW) or 192 kWh (at a thermal load of 8 kW) is withdrawn from the thermal energy storage in a period of 24 h, both for the constant and the variable load profile.

Parameter C describes the positions of the temperature sensors used for the control of the CHP unit in heat-led mode, as explained in Section 3. For the minimum setting, the two sensors T_{middle} and T_{lower} are used in this respect. Fig. 3 reveals that in this case only a small part of the total volume of the tank is involved in the process of storing thermal energy. The CHP unit is turned on whenever the temperature in the tank falls below a set point of 60 °C at the middle sensor, and it is turned off as soon as the set-point temperature of 60 °C is exceeded at the lower sensor.

In contrast, in the maximum setting, the CHP unit is turned off when the temperature set-point of 60 °C is exceeded in the return line to the CHP unit. In this way, the thermal energy storage can be charged completely, which is not possible in case of the minimum setting, since there will be always cold water from the return line of the heating system at the bottom of the tank. The command for turning the CHP unit on is again determined based on the middle temperature sensor. Hence, the CHP is turned on whenever the temperature at the middle sensor drops below the set-point of 60 °C. For the maximum setting, the upper temperature sensor on the storage tank could also have been selected for this purpose; however, the middle sensor has been chosen in the course of this analysis so that the tests at the minimum and maximum settings are congruent on this point.

As mentioned before, the parameter variation is carried out within the framework of a statistical experimental design, in order to characterise the effect of each parameter on the performance of the thermal energy storage. For this purpose, the method of Yates is applied [28]. Specifically, it involves an experimental design comprising three factors to be analysed, namely thermal load, thermal load profile, and sensor position with two stages. Regarding to Yates this yields an experimental plan with eight experiments. Accordingly, the main effects for the three factors can be reliably determined as well as the 2-factor interactions. In addition, the 3-factor interaction can be analysed, which, however, is very small in many applications. Table 3 shows the parameter combinations for the eight tests, where the actual values are entered and the information maximum/minimum value is given by the colours green for maximum and orange for minimum value.

Table 3
Parameter variation according to the 3-factor DOE.

Factor	A	B	C
Experiment	Thermal load	Thermal load profile	Sensor position
E1	3 kW	Constant	T_{middle}/T_{lower}
E2	8 kW	Variable	T_{middle}/T_{lower}
E3	3 kW	Variable	T_{middle}/T_{CHP2}
E4	8 kW	Constant	T_{middle}/T_{CHP2}
E5	3 kW	Constant	T_{middle}/T_{CHP2}
E6	8 kW	Variable	T_{middle}/T_{CHP2}
E7	3 kW	Variable	T_{middle}/T_{lower}
E8	8 kW	Constant	T_{middle}/T_{lower}

6. Results and discussion

This section is divided into two major parts that focus on the results for effective capacity and thermal stratification, respectively. Firstly, a brief description of the experimental results is provided with a focus on experiment 7. This is done to highlight what the measured results look like for an experiment with a variable load profile before the analysis of the experimental data is further discussed.

Fig. 5 shows a set of results from experiment 7 with a variable load with 3 kW mean and TES sensor positions T_{middle} and T_{lower} (see Table 3 in Section 5). The figure visualises the measured flow rates in the CHP and the space heating circuit, and the temperatures at different heights within the TES. Fig. 5(a) illustrates the variable load, which was applied in experiment 7, by the variable flow rate in the space heating circuit. With respect to the time on the x-axis, it can be seen that a daily profile has been implemented starting at midnight with two peaks in the space heating demand, one in the morning around 7:00 and the other one the evening around 20:00. This profile was repeated every 24 h for a total duration of 3 days. The same experimental duration has been applied to the other experiments listed in Table 3. The flow rate in the CHP circuit in Fig. 5(a) clearly shows the On/Off-operation of the CHP unit. Whenever the CHP unit is off, there is no flow rate, since the pump in the circuit is off as well. In contrast, during times of CHP operation the flow rate in the CHP circuit varies between 3 and 3.7 litres/min.

The On/Off-operation of the CHP unit is also visible from the variation of the temperatures in the TES, as seen in Fig. 5(b). TES temperatures rise during the times of CHP operation indicating that the TES is charged, and temperatures decline in the periods where the CHP unit is off, representing the discharging cycles. Moreover, the temperature distribution over the height of the tank is visible in the data from sensors $TC1$–$TC7$ attached to the tank at different heights as shown in Fig. 3. It can be seen that the major fluctuations in temperature occur in layers 1 to 3 in the lower and middle sections of the tank. This is attributed to the fact that in experiment 7 temperature sensor T_{middle} is used for indicating that the TES is fully charged. For that reason, the section of the tank above sensor T_{middle} does not actively take part in the process of storing thermal energy, which already implies that the positions of the sensors for turning the CHP unit on and off strongly affect the effective capacity of the TES. Finally, Fig. 5(b) reveals how the temperatures approach a constant amplitude oscillation during the course of the experiment. Evidently, the amplitude of the oscillation does not become entirely constant, which is caused by the variable load profile.

Finally, Fig. 5(c) illustrates the cyclic behaviour of the temperature sensors for turning the CHP unit on and off, T_{lower}, T_{middle} and T_{upper}. Comparing to 5(b) it can be seen that the temperatures correspond to the data collected from the thermocouple sensors located at the same height of the tank. Namely, the data of sensor T_{lower} coincides with $TC1$ at the bottom of the tank. Accordingly, the temperatures of sensor T_{upper} corresponds to the data of thermocouple sensor $TC5$, while the temperature curve of sensor T_{middle} finds itself between thermocouple sensor $TC3$ and $TC4$ (compare to Fig. 3). It should be noted that the temperatures of sensor T_{CHP2} are not displayed in Fig. 5(c), since the data is not meaningful. The reason for this is that the sensor is located in the return line to the CHP unit, which does not show any flow when the CHP unit is switched off. Consequently, the temperature values in these phases are not relevant.

6.1. Results for TES effective capacity

As outlined before, the positions of the sensors that are used for turning the CHP unit on and off strongly impact TES effective capacity. Fig. 6 reveals the significant difference in TES effective capacity when the middle temperature sensor and the CHP return line temperature sensor T_{middle}/T_{CHP2} are used compared to when the middle and lower temperature sensors T_{middle}/T_{lower} are used. Therefore, the tank volume between the two sensors for turning the CHP unit on and off is larger for experiments with sensor positions T_{middle}/T_{CHP2} resulting in a higher effective capacity. For that reason, it is recommended to separate the two sensors for switching the CHP unit as much as possible, in order to push the effective thermal capacity of a TES as best as possible to its physical limit, which is given by the total volume of the tank.

The effects of the other two parameters that were varied, namely the thermal load and the thermal load profile, on the TES effective capacity are comparatively small. However, the results in Fig. 6 show that all experiments with a variable thermal load (represented by the hatched bars) show slightly higher values for effective capacity compared to the experiments with a constant thermal load (represented by the full bars) under the same conditions. Hence, the load profile shows a small but significant effect on TES effective capacity. In contrast, the effect of thermal load itself is insignificant. Fig. 6 reveals that the experiments with a thermal load of 3 kW (orange bars) show slightly higher TES effective capacities compared to the tests at 8 kW (green bars) in case of sensor positions T_{middle}/T_{lower}; but in case of sensor positions T_{middle}/T_{CHP2} a reversed effect is visible.

6.2. Results for thermal stratification

As previously outlined, thermal stratification is given by the separation of hot water travelling to the top of the tank due to its lower density compared to cold water, which for that reason tends to fall to the bottom of the tank. Hence, thermal stratification may be visualised best in a plot of temperature versus height of the tank, where the height is displayed on the vertical axis and the temperature in the tank on the horizontal axis. Such plots are given in Fig. 7 for experiment 3 on the left and experiment 7 on the right. Experiments 3 and 7 were selected in order to highlight the effect of sensor positions at constant conditions regarding the other two varied parameter. The temperatures of the water in the tank are taken from sensors $TC1$–$TC7$, and they are marked by small crosses. The different curves displayed in Fig. 7 refer to the time instants where the CHP unit is turned on (blue curves on the left of each diagram) and the time instants where the CHP unit is turned off (red curves on the right of each diagram). Evidently, the times where the CHP unit is turned on correspond to a “fully discharged” TES, and the times where the CHP unit is turned off correspond to a “fully charged” TES. In addition, both Figures show the position of the switching sensors T_{middle} and T_{lower}. It can be seen that in case of experiment 7 (Fig. 7(b)) all (blue) curves for turning the CHP unit on meet in one point marked by the position of the relevant sensor T_{middle}. The same can be observed for the instant when the CHP unit is turned off: All (red) curves meet in one point marked by the position of sensor T_{lower}. The same characteristics refer to Fig. 7(a) on the left with the only difference that in case of experiment 3 the sensor for turning the CHP unit off, T_{CHP2}, is located outside of the tank, and it can for that reason not be displayed in the diagram.

Fig. 7(b) on the right shows the temperature curves for 15 On/Off-cycles during the 72 h of experiment 7, and the transient response is

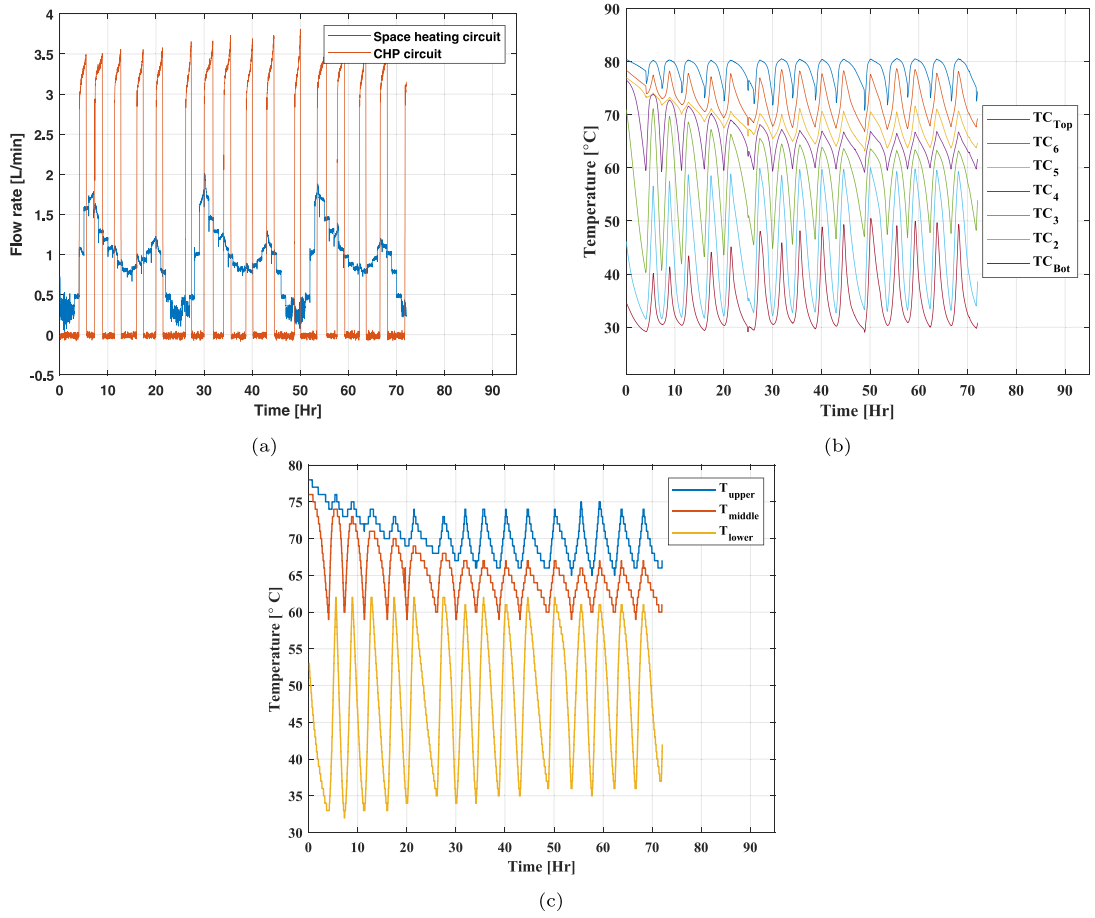

Fig. 5. (a) Measured data for flow rates in the CHP and the space heating circuit, (b) the temperatures at different heights within the TES as a function of time for experiment 7 and (c) the switching temperatures at the upper, middle, and lower locations of the TES buffer tank.

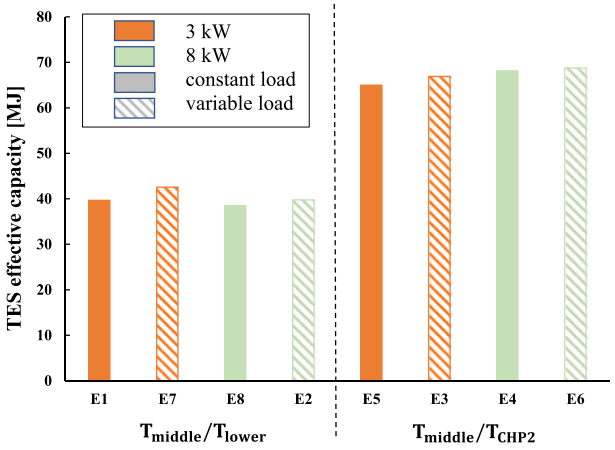

Fig. 6. TES effective capacity according to Eq. (3) for experiments 1–8.

clearly evident. It can be seen that thermal stratification in the TES deteriorates as the number of cycles increases. At the beginning of the experiment, the temperature curves are rather vertical at the upper and lower ends of the tank, while the incline in the centre of the tank is rather flat. As the number of On/Off-cycles increases, almost linear temperature curves occur with a mixing zone that extends over almost the entire tank. In addition, it can be seen that the variation of the temperature curves diminishes cycle by cycle, and a quasi steady state is reached at the end of the experiment.

In contrast, the temperature curves displayed in Fig. 7(a) on the left show only very small variations. Hence, thermal stratification is quite stable in time compared to experiment 7. The reason for this behaviour is the different position of the sensors for turning the CHP unit on and off. More precisely, this effect is caused by the position of the sensor for turning the CHP unit off in experiment 3, sensor T_{CHP2}, since it is located in the return line to the CHP unit and therefore outside of the tank. For this reason, the higher temperatures from the supply line of the CHP unit are able to reach the bottom of the tank. Fig. 7(a) clearly shows that at the time instants when the CHP unit is turned off, the temperatures in the bottom of the tank vary between 65 and 70 °C. In experiment 7, where sensor T_{lower}, which is located inside the tank, is used for turning the CHP unit off, the temperatures in the bottom vary between 40 and 48 °C (see Fig. 7(b)), and they approach the return temperature from the space heating circuit even lower in the tank. In other words, with the temperature sensor for turning the CHP unit off located outside of the tank, the entire zone of thermal stratification is flushed out of the tank. As a result, after the CHP unit turns off, stratification is rebuilt by the cold water entering from the return line of the space heating circuit. In this way, thermal stratification cannot deteriorate over time due to mixing, diffusion and heat conduction processes as observed for experiment 7 in Fig. 7(b). Obviously, the same result could be achieved by locating the sensor for turning the CHP unit on from the top of the tank to the outside of the tank in the supply line for the heating circuit. Hence, it is recommended to place at least one of the two sensors for turning the CHP unit on and off outside of the TES tank. However, following the recommendation from the previous section, the TES effective capacity will be maximised if both sensors are located outside of the tank.

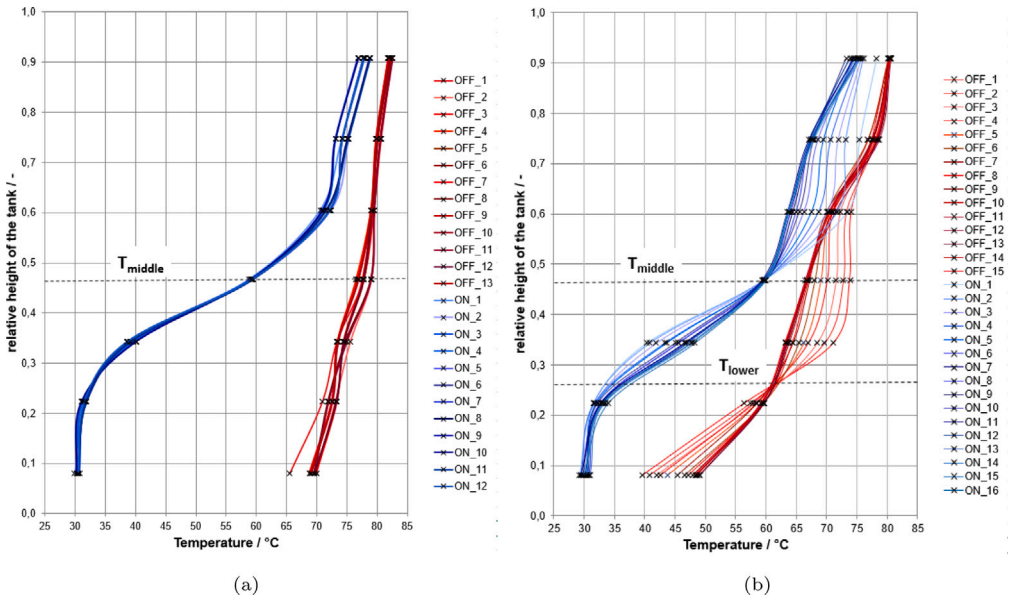

Fig. 7. Temperature distribution in the TES as a function of relative height at the time incidents of the CHP unit turning on (blue curves corresponding to TES "fully discharged") and the CHP turning off (red curves corresponding to TES "fully charged") for experiment 3 on the left and experiment 7 on the right.

As the results presented so far revealed that thermal stratification in the TES varies between the different experiments and, in addition, is a function of time, the next section of the paper is dedicated to the thermodynamic analysis of thermal stratification by the metrics introduced in Sections 4.3 and 4.4. Fig. 8 shows the variation of the different metrics in time for experiment 3 on the left and experiment 7 on the right. On the one hand, the oscillation caused by the charging and discharging cycles is clearly visible. On the other hand, the different behaviour between experiment 3 and experiment 7, as observed before with the help of Fig. 7, is evident again.

For experiment 7, which is characterised by sensor positions $T_{\mathrm{middle}}/T_{\mathrm{lower}}$, the deterioration of thermal stratification as discussed before can also be seen as the curves tend to fall and approach smaller values during the 72 h period of the experiment. Note that only the MIX number shows higher values in cases where the stratification deteriorates. For that reason the modified number MIX* was introduced in Section 4.3.5. In contrast, for experiment 3, representing sensor positions $T_{\mathrm{middle}}/T_{\mathrm{CHP2}}$, the oscillation is almost constant indicating that thermal stratification does not deteriorate but is stable instead, as explained before. However, the data always approaches a steady state if a low frequency moving average is applied as depicted by the dashed lines in the plots of Fig. 8. From these results it can be noted that there are small disturbances in the moving average, closer to the end of the data. These have been characterised as edge effects of the moving average algorithm. However, these edge effects occur after the trend has reached steady-state. These steady state values are captured in Table 4 and displayed in Fig. 9, shown at the end of this section, and as bar graph plots for the different metrics and the eight experiments, which will be discussed next.

Overall, experiments representing sensor positions $T_{\mathrm{middle}}/T_{\mathrm{CHP2}}$ always show higher numbers compared to experiments based on sensor positions $T_{\mathrm{middle}}/T_{\mathrm{lower}}$. This result confirms the conclusion from the previous paragraphs, where it was found by analysing the temperature plots for experiments 3 and 7 that no deterioration of stratification occurs, if one of the two sensors for turning the CHP unit on and off is located outside of the TES tank. Moreover, this conclusion can be reproduced for all experiments, and it can be assessed by all four metrics suggested for evaluating thermal stratification thermodynamically.

Hence, a significant effect of sensor position on the thermodynamic quality of thermal stratification with respect to MIX* number, stratification number exergy number and exergy efficiency can be postulated in a way that locating one of the two sensors for turning the CHP unit on and off outside of the tank enhances thermal stratification in the TES.

For analysing the effects of the two other parameters, namely thermal load and thermal load profile, the bar plots of the different metrics are analysed individually. Note that the numerical values for the bar plots are given as supplemental information in Table 4 at the end of this section.

Starting with the normalised stratification factor ST* in Fig. 9(a), it can be seen that a higher thermal load results in a higher stratification factor ST* and therefore in a better quality of thermal stratification. For that reason the effect of thermal load on stratification factor ST* should be considered as significant. Moreover, the data displayed in Fig. 9(a) reveals that the impact on ST* is higher for sensor positions $T_{\mathrm{middle}}/T_{\mathrm{lower}}$ compared to $T_{\mathrm{middle}}/T_{\mathrm{CHP2}}$. In contrast, the effect of thermal load profile on stratification factor ST* cannot be identified explicitly. Only in case of sensor positions $T_{\mathrm{middle}}/T_{\mathrm{CHP2}}$ and a high thermal load of 8 kW a variable thermal load tends to reduce stratification factor ST*. For all other variations the effect of thermal load on ST* is very small and in the range of the uncertainties of the analysis. For that reason, based on the experiments in the course of this paper no evidence could be found for this effect.

The results of the MIX* number are visualised in Fig. 9(b) and they show the same trends as previously revealed for the normalised stratification factor ST*. In terms of thermal load, Fig. 9(b) illustrates that the MIX* number for the experiments with a higher thermal load of 8 kW always exceed the numbers of the experiments with a smaller thermal load of 3 kW. For that reason, this effect can be considered significant. In other words, a higher thermal load yields a better quality of stratification if the MIX* number is used as the descriptive metric. The effect of thermal load profile on MIX* number is not evident. Again, only for sensor positions $T_{\mathrm{middle}}/T_{\mathrm{CHP2}}$ and a high thermal load of 8 kW a variable thermal load tends to result in a reduction of the MIX* number. All other variations show insignificant changes of the MIX* number as a function of thermal load profile.

The results for the exergy analysis, as expressed by the exergy number Ex* and the exergy efficiency η_{Ex}, are plotted in Figs. 9(c) and 9(d), respectively. By comparing the results for exergy number Ex* to normalised stratification factor ST* and MIX* number in Figs. 9(a) and 9(c) it is evident that the exergy number shows the same trends as explained previously. Again, the variation of Ex* with thermal load

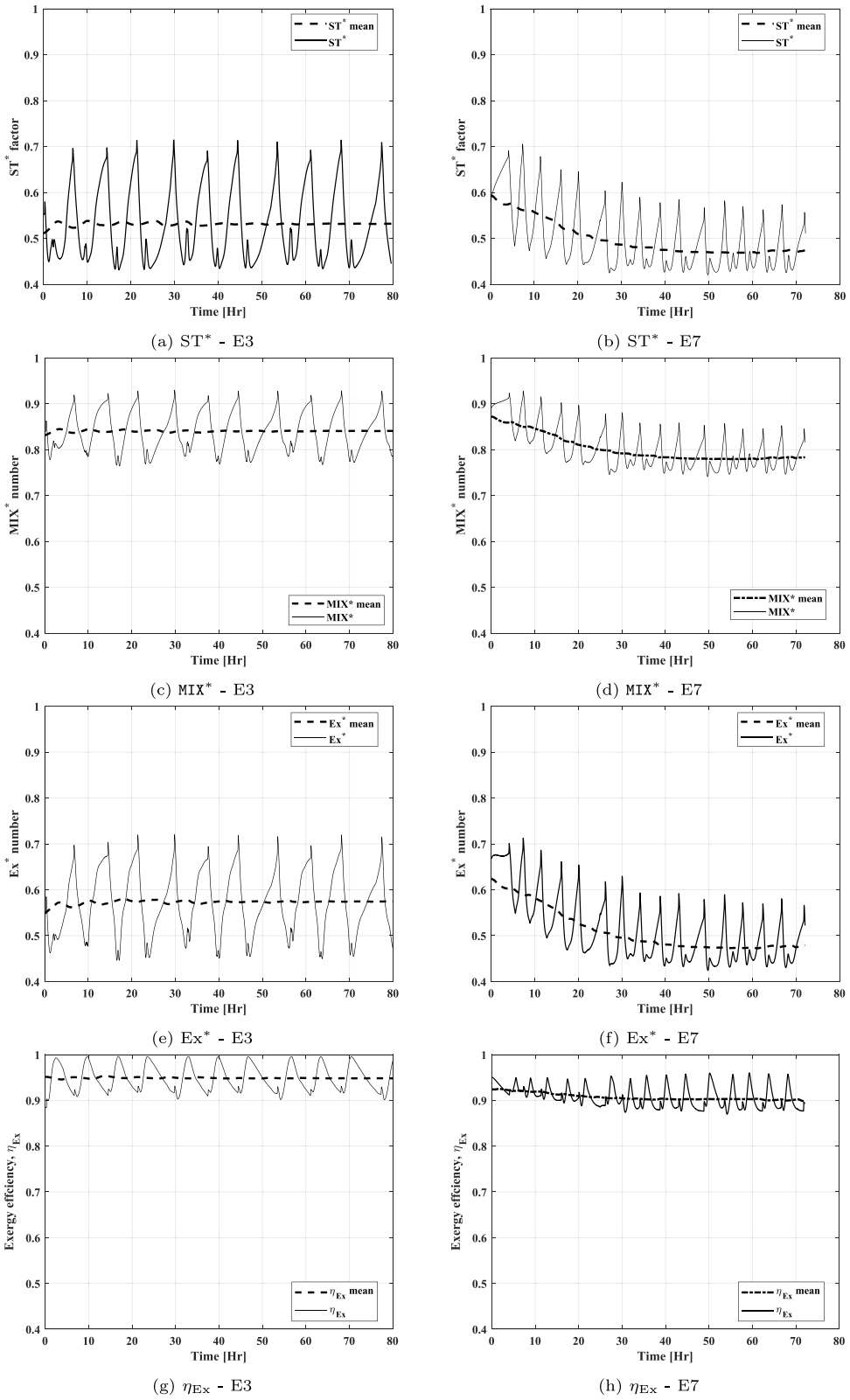

Fig. 8. Time-series results for all relevant performance metrics to characterise thermal stratification for experiments 3 (E3) and 7 (E7). Results for E3 are presented in the left column and results from E7 in the right. The black solid lines represent the cyclic behaviour of the TES whereas the dark dashed lines represent a low frequency moving average of the cyclic behaviour as seen in each figure. All scales are between 0.4 and 1 for better visual comparison.

profile is very small. Hence, no clear effect can be observed. Instead, it can be stated that exergy number is independent of thermal load profile in the course of the experiments discussed in this paper. In contrast, the magnitude of the thermal load significantly affects the exergy number Ex^* in the same way as discovered for normalised stratification factor ST^* and MIX^* number. Thus, it can be concluded that a higher thermal load yields a higher exergy number and therefore a better quality of thermal stratification in terms of exergy. Finally, the exergy efficiency

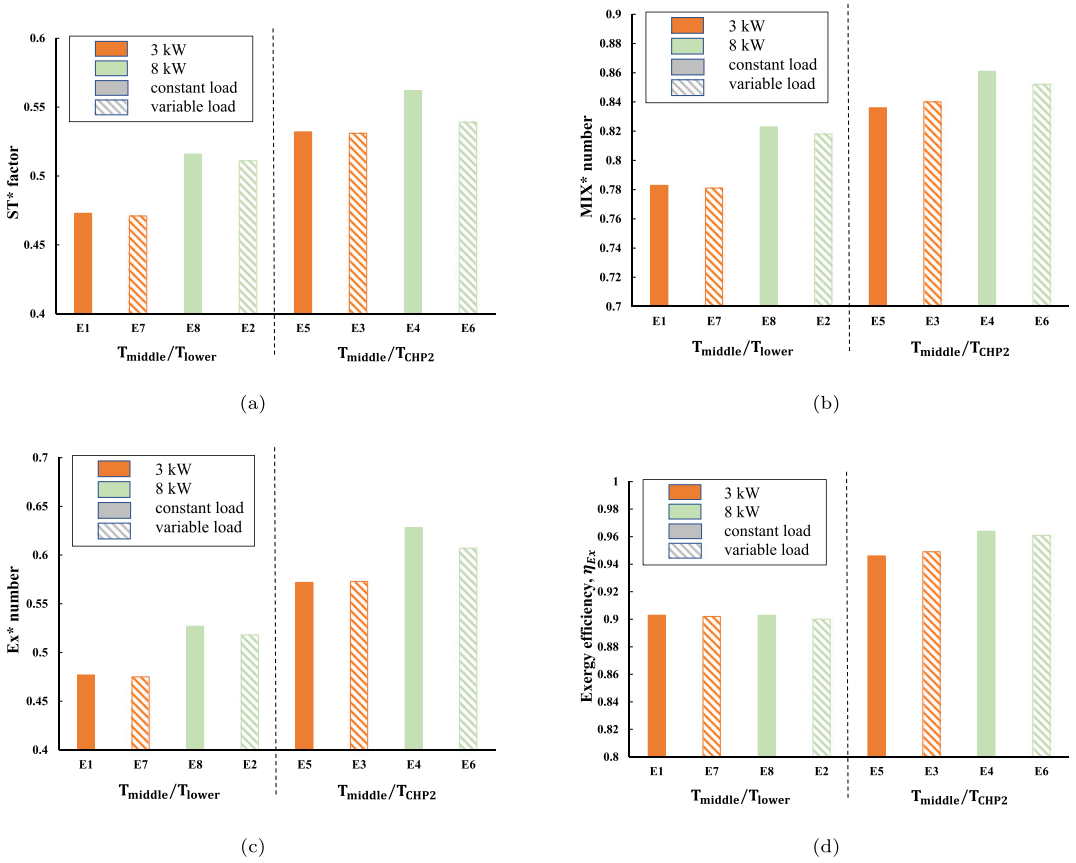

Fig. 9. Evaluation of stratification for all eight experiments based on the metrics (a) normalised stratification factor ST*, (b) MIX* number, (c) exergy number Ex* and (d) exergy efficiency η_{Ex} as derived in Section 4. Note that different scales are applied to the vertical axes of the subplots.

η_{Ex} also follows these trends, which is not surprising, because exergy efficiency η_{Ex} and exergy number Ex* are closely related. However, due to the definition of exergy efficiency the range of this metric covers values between 0.9 and 0.97, which is quite narrow. Consequently, the trends are not as clearly visible as it is the case for exergy number, where the span between the extreme values ranges between 0.48 and 0.62. Therefore, using exergy number Ex* instead of exergy efficiency η_{Ex} could be considered to be more convenient for identifying any trends of thermal stratification on the exergy content of a TES.

Following the discussion of the results for the different metrics, it is clear to note the close connection between thermal stratification and thermodynamic effectiveness of a TES. While normalised stratification factor ST* and MIX* number are defined for describing the quality of thermal stratification, exergy number Ex* and exergy efficiency η_{Ex} express the thermodynamic effectiveness of any thermodynamic system. Since the analyses prove that all the applied metrics show the same trends with respect to the parameter variation applied in the experiments, it can finally be concluded that a high quality of thermal stratification in a TES tank is a distinctive identifier for its higher thermodynamic effectiveness.

7. Conclusion

This paper aimed to analyse thermal stratification in a TES as part of a cogeneration plant. Different parameters like thermal load, thermal load profile and the position of the temperature sensors that are used for turning the CHP unit on and off in heat-led mode were varied in eight experiments. The effects on thermal stratification in the TES as well as on the TES effective capacity were extracted from the experimental results. In summary, three major findings resulted from the analysis presented in this paper so far:

Table 4
Numerical results of analyses. The values in this table are recorded from the stabilised, steady-state moving average near the end of the experiment for each calculated metric, as seen in Fig. 8.

Experiment	ST*	MIX*	Ex*	η_{Ex}	[a]$Q_{TES,eff}$
E1	0.473	0.783	0.477	0.903	39.71 MJ
E2	0.511	0.818	0.518	0.900	39.77 MJ
E3	0.531	0.840	0.573	0.949	66.89 MJ
E4	0.562	0.861	0.628	0.964	68.14 MJ
E5	0.532	0.839	0.572	0.946	64.97 MJ
E6	0.539	0.852	0.607	0.961	68.76 MJ
E7	0.471	0.781	0.475	0.902	42.58 MJ
E8	0.516	0.823	0.527	0.903	38.52 MJ

[a]Refer to Fig. 6

1. TES effective capacity strongly depends on positions of the sensors used for controlling the CHP unit
2. For preventing deterioration of thermal stratification over time, at least one of the sensors for controlling the CHP unit should be placed outside of the TES tank.
3. A high quality of thermal stratification is equivalent to a high thermodynamic effectiveness in a vertically oriented TES tank.

Regarding the first finding, the results from the experiments confirmed that only the volume between the two sensors for turning the CHP unit on and off is actively involved in the charging and discharging process. Therefore, it is recommended to refer to this volume when determining the energetic capacity of a TES instead of the nominal volume of the tank serving as TES. The two other parameters that were varied, namely the thermal load and the thermal load profile, showed much smaller effects on the TES effective capacity. However, the effect

of the thermal load profile is significant in that a variable thermal load yields slightly higher values for the TES effective capacity compared to a constant thermal load. In contrast, the effect of the size of the thermal load on the TES effective capacity was found to be negligible.

The second finding of the paper results from the analysis of the temperature distribution in the TES over time. It was observed that thermal stratification in the TES deteriorates over time due to mixing, diffusion and heat conduction processes. However, a quasi-steady state was reached after a reasonable number of charging and discharging cycles. In order to prevent this effect, which evidently reduces thermodynamic effectiveness of the TES, at least one of the two temperature sensors for turning the CHP unit on and off should be placed outside of the TES tank. By this means, in each cycle where the sensor outside of the tank is involved the stratification zone is completely flushed out of the tank, and by starting the new cycle thermal stratification rebuilds anew.

The analysis of stratification quality by the metrics elaborated beforehand, such as normalised stratification factor ST^*, MIX^* number, exergy number Ex^* and exergy efficiency η_{Ex}, confirm the effect of the sensor positions. All metrics show higher values indicating a higher thermodynamic effectiveness in the case where the sensor for turning the CHP unit off is placed in the return line to the CHP unit and by this means outside of the tank instead of locating it in the tank. Moreover, it was found that thermal load profile does not affect stratification at all, while a higher thermal load tends to increase the quality of thermal stratification slightly. In comparison, all four metrics applied show the same effects on thermal stratification regarding the varied parameter thermal load, thermal load profile and sensor positions. Hence, either of these metrics can be used to evaluate thermal stratification of a TES as part of a cogeneration unit. In other words, a good quality of thermal stratification expressed by high numbers for ST^* and MIX^* is equivalent to a high thermodynamic effectiveness of the TES tank given by large values for exergy number Ex^* and exergy efficiency η_{Ex}. The good applicability of exergy for evaluating thermal stratification has already been proposed by Celador, et al. [15]. In contrast and as outlined in Section 4.5, Peclet number and Richardson number cannot handle more than one outlet and one inlet port at the TES. For that reason, the definition of these metrics needs to be extended for applying them to a TES in CHP installations. This result coincides with the findings of Castell, et al. [13]; they also concluded that Peclet number is not suitable for characterising thermal stratification. Stratification number is as well not suited to evaluate thermal stratification in such installations, because it lacks the effect of temperature distribution following the definition from Section 4.3.1.

In view of practical installations, it can be concluded from the work presented here that the potential of a TES can be better implemented by an appropriate integration, especially with regard to the positioning of the temperature sensors. The insight provided by the analysis of the temperature profiles in the TES as well as by applying the metrics for evaluating thermal stratification quality reinforce this endeavour. Moreover, the results should be understood as a prologue to further investigations, which are certainly necessary for a better understanding of the conditions and processes affecting thermal stratification and consequently, the thermodynamic effectiveness of a TES device. In this context, the transferability to other sizes and geometries should be investigated as well as the effects of other parameters.

Declaration of competing interest

The authors declare the following financial interests/personal relationships which may be considered as potential competing interests: MJ BOOYSEN reports financial support was provided by MTN South Africa.

Data availability

Data will be made available on request.

References

[1] United Nations - Framework Convention on Climate Change (FCCC), Adoption of the Paris agreement, 2015, URL: https://unfccc.int/resource/docs/2015/cop21/eng/l09r01.pdf.

[2] United Nations - Framework Convention on Climate Change (FCCC), Report of the conference of the parties serving as the meeting of the parties to the Paris agreement on its third session, held in Glasgow from 31 October to 13 November 2021, 2021, URL: https://unfccc.int/sites/default/files/resource/cma2021_10_add1_adv.pdf.

[3] European Commission, European Green Deal: Commission proposes transformation of EU economy and society to meet climate ambitions, 2021, URL: https://ec.europa.eu/commission/presscorner/detail/en/IP_21_3541.

[4] The White House, FACT SHEET: President Biden sets 2030 greenhouse gas pollution reduction target aimed at creating good-paying union jobs and securing U.S. leadership on clean energy technologies, 2021, URL: https://www.whitehouse.gov/briefing-room/statements-releases/2021/04/22/fact-sheet-president-biden-sets-2030-greenhouse-gas-pollution-reduction-target-aimed-at-creating-good-paying-union-jobs-and-securing-u-s-leadership-on-clean-energy-technologies/.

[5] D. Sandalow, M. Meidan, P. Andrews-Speed, A. Hove, S.Y. Qiu, E. Downie, Guide to Chinese climate policy 2022, 2022, URL: https://chineseclimatepolicy.oxfordenergy.org/wp-content/uploads/2022/11/Guide-to-Chinese-Climate-Policy-2022.pdf.

[6] A. Toradmal, T. Kemmler, B. Thomas, Boosting the share of onsite PV-electricity utilization by optimized scheduling of a heat pump using buildings thermal inertia, Appl. Therm. Eng. 137 (2018) 248–258, URL: https://www.sciencedirect.com/science/article/pii/S1359431117359902.

[7] P. Haase, B. Thomas, Test and optimization of a control algorithm for demand-oriented operation of CHP units using hardware-in-the-loop, Appl. Energy 294 (2021) 116974, URL: https://www.sciencedirect.com/science/article/pii/S0306261921004487.

[8] M.Y. Haller, C.A. Cruickshank, W. Streicher, S.J. Harrison, E. Andersen, S. Furbo, Methods to determine stratification efficiency of thermal energy storage processes - Review and theoretical comparison, Sol. Energy 83 (2009) 1847–1860.

[9] P. González-Altozano, M. Gasque, F. Ibáñez, R.P. Gutiérrez-Colomer, New methodology for the characterisation of thermal performance in a hot water storage tank during charging, Appl. Therm. Eng. 84 (2015) 196–205.

[10] M. Gasque, F. Ibáñez, P. González-Altozano, Minimum number of experimental data for the thermal characterization of a hot water storage tank, Energies 14 (2021).

[11] J. Fernández-Seara, F.J. Uhía, J. Sieres, Experimental analysis of a domestic electric hot water storage tank. Part II: Dynamic mode of operation, Appl. Therm. Eng. 27 (2007) 137–144.

[12] Y.P. Chandra, T. Matuska, Stratification analysis of domestic hot water storage tanks: A comprehensive review, Energy Build. 187 (2019) 110–131.

[13] A. Castell, M. Medrano, C. Solé, L.F. Cabeza, Dimensionless numbers used to characterize stratification in water tanks for discharging at low flow rates, Renew. Energy 35 (2010) 2192–2199.

[14] P.D. van Schalkwyk, J.A.A. Engelbrecht, M.J. Booysen, Thermal stratification and temperature variation in horizontal electric water heaters: A characterisation platform, Energies 15 (2022).

[15] A. Campos Celador, M. Odriozola, J.M. Sala, Implications of the modelling of stratified hot water storage tanks in the simulation of CHP plants, Energy Convers. Manage. 52 (2011) 3018–3026.

[16] Z. Wang, H. Zhang, B. Dou, H. Huang, W. Wu, Z. Wang, Experimental and numerical research of thermal stratification with a novel inlet in a dynamic hot water storage tank, Renew. Energy 111 (2017) 353–371.

[17] M.N.I. Maruf, G. Morales-España, J. Sijm, N. Helistö, J. Kiviluoma, Classification, potential role, and modeling of power-to-heat and thermal energy storage in energy systems: A review, Sustain. Energy Technol. Assess. 53 (2022) arXiv:2107.03960.

[18] F. Lai, S. Wang, M. Liu, J. Yan, Operation optimization on the large-scale CHP station composed of multiple CHP units and a thermocline heat storage tank, Energy Convers. Manage. 211 (2020) 112767.

[19] Z. Wang, Y. Gu, S. Lu, Z. Zhao, Optimization of thermocline heat storage tank capacity for combined heat and power plant based on environmental benefits: Scenarios for China, J. Energy Storage 57 (2023) 106303.

[20] C. Kizilors, D. Aydin, Effect of thermostat position and its set-point temperature on the performance of a domestic electric water heater, Int. J. Low-Carbon Technol. 15 (2021) 373–381.

[21] A.A. Farooq, A. Afram, N. Schulz, F. Janabi-Sharifi, Grey-box modeling of a low pressure electric boiler for domestic hot water system, Appl. Therm. Eng. 84 (2015) 257–267.

[22] O. Abdelhak, H. Mhiri, P. Bournot, CFD analysis of thermal stratification in domestic hot water storage tank during dynamic mode, Build. Simul. 8 (2015) 421–429.

[23] Y.P. Chandra, T. Matuska, Numerical prediction of the stratification performance in domestic hot water storage tanks, Renew. Energy 154 (2020) 1165–1179.

[24] P. Kepplinger, G. Huber, M. Preißinger, J. Petrasch, State estimation of resistive domestic hot water heaters in arbitrary operation modes for demand side management, Therm. Sci. Eng. Prog. 9 (2019) 94–109.
[25] J. Fernández-Seara, F.J. Uhía, J. Sieres, Experimental analysis of a domestic electric hot water storage tank. Part I: Static mode of operation, Appl. Therm. Eng. 27 (2007) 129–136.
[26] O. Abdelhak, H. Mhiri, P. Bournot, CFD analysis of thermal stratification in domestic hot water storage tank during dynamic mode, Build. Simul. 8 (2015) 421–429.
[27] L. Wu, R. Bannerot, Experimental study of the effect of water extraction on thermal stratification in storage, in: ASME-JSME-JSES Solar Energy Conference, Honolulu, 1987, pp. 445–451.
[28] G.E.P. Box, W.G. Hunter, W.G. Hunter, J.S. Hunter, Statistics for Experimenters an Introduction to Design, Data Analysis, and Model Building, J. Wiley, 1978.